Journal of Structural Geology, Vol 13, No 9, pp 1049 to 1059, 1991
Printed in Great Britain

0191-8141/91 $03 00+0.00

Three-dimensional finite strain from crinoid ossicles

MARK G ROWAN*

Department of Geological Sciences, Campus Box 250, University of Colorado, Boulder, CO 80309, U S A

(Received 5 October 1990, accepted in revised form 2 April 1991)

Abstract—Randomly oriented crinoid ossicles are useful markers for the determination of three dimensional finite strain Two techniques are presented Both make use of established methods to measure the two dimensional strain ellipses on three surfaces, which are then combined to calculate the shape and orientation of the strain ellipsoid First, ossicles positioned such that a thin section cuts across the cylinder appear as randomly oriented ellipses prior to deformation, and can be analyzed using standard R_f/ϕ methods Second, ossicles positioned such that the section cuts lengthwise through the cylinder appear as rectangular or sub rectangular shapes with orthogonal geometries in the undeformed state. Measurements of angular shear strain on two or more such markers are analyzed using a non linear least squares solution to the Breddin graph, allowing determination of the best fit strain ellipse

Both methods are applied to an echinoderm grainstone from the central Helvetic nappes of Switzerland The results are internally consistent, and compatible with those from other strain analysis techniques

INTRODUCTION

IN HIS seminal publication on oolite deformation in the South Mountain fold, Cloos (1947, pp. 892–894) suggested that crinoid stems could be used to evaluate and quantify strain in naturally deformed rocks He recognized that crinoid disks, or ossicles, often are deposited parallel to bedding, and that since the ossicles are initially circular in cross section, the shape and orientation of the strain ellipse in the bedding plane can be measured directly He also illustrated that three dimensional strain can be calculated in favorable circumstances, namely when whole crinoid stems lying within bedding are oriented parallel to the principal finite strain axes. In practice, however, these conditions are rarely satisfied, and crinoids generally have been used to quantify only the two dimensional strain within the bedding plane (Hellmers 1955, Breddin 1956a,b, Kurtman 1960, Nissen 1964, Engelder & Engelder 1977, Faill 1977, Engelder 1979, Oertel *et al* 1989)

Two sources of potential error in the simple two-dimensional analysis are related to the assumption of initial circular shape of the ossicles. First, although most crinoid stems are indeed circular in cross section, several species have originally elliptical profiles (Nissen 1964, Moore & Teichert 1978, Spratt 1987). Second, even for initially circular ossicles, the technique is applicable only if the disks are truly parallel to bedding; if they are not, the undeformed profile in the bedding plane is elliptical (Engelder & Engelder 1977, Spratt 1987) In both these cases, the measured ossicle shape and orientation are not those of the strain ellipse, but rather those of the combined effect of the initial form and the strain ellipse. A related problem was pointed out by Ramsay (1967, pp. 229–230), who demonstrated that a cross section perpendicular to the axis of a deformed cylinder generally does not represent the strain ellipse, as it usually is derived from an oblique, elliptical cut through the undeformed cylinder.

Spratt (1987), in a detailed analysis of deformation mechanisms within crinoidal limestones of the Canadian Rockies, acknowledged and addressed these problems First, she documented that the ossicles were initially circular by measuring the shapes of relatively undeformed samples. Second, by microscopically determining the orientation of the c axis of each crinoid stem (which forms a single calcite crystal), she was able to calculate and remove the effects of oblique cuts through ossicles, and thus specify both the original ellipticity of the cut and the true strain ellipse. Since this is applicable to ossicles and thin sections of any orientation, her technique allows the three dimensional strain to be calculated, as long as the undeformed cross sectional shapes are known.

In this contribution, two new methods are presented for determining the three-dimensional strain from crinoid ossicles Like the technique of Spratt (1987), both are applicable to rocks, typically crinoidal grainstones, in which ossicles are randomly oriented. Furthermore, both methods make use of the two-dimensional shapes created by thin sections cutting the three dimensional cylindrical ossicles; these shapes can be evaluated by the standard R_f/ϕ (e g. Ramsay 1967, pp. 202–211, Dunnet 1969, Lisle 1977) and angular shear strain (Breddin 1956a, Ramsay 1967, pp 236–242) techniques. The three dimensional strain is calculated from measurements of two dimensional strain on three mutually perpendicular sections (Ramsay 1967, pp. 142–147, Siddans 1980) or three or more non perpendicular sections (Owens 1984) Two advantages of these new methods over that developed by Spratt (1987) are that the c axis orientations need not be determined, and knowledge of the original shape of the ossicles is not required.

*Present address, Alastair Beach Associates, 11 Royal Exchange Square, Glasgow G1 3AJ, U K

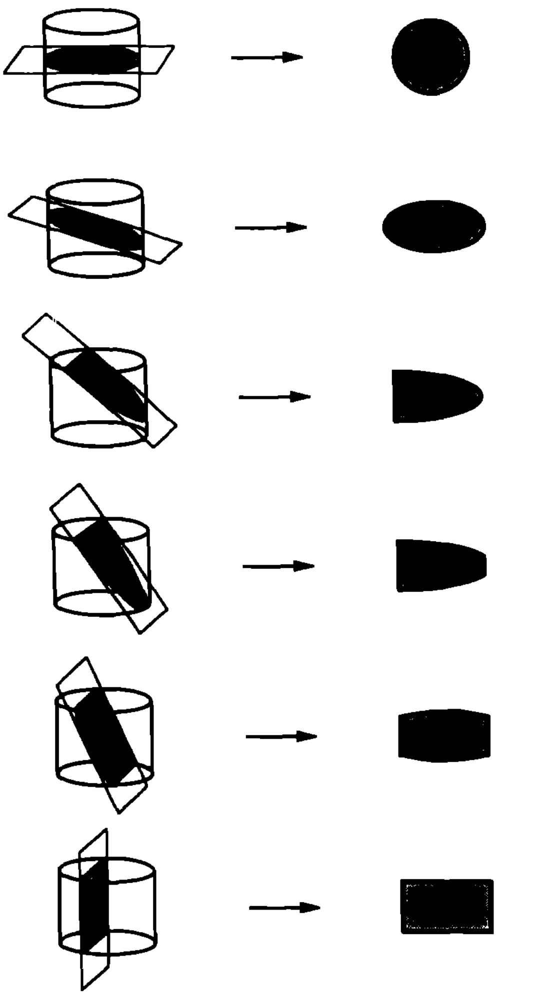

Fig. 1. Two dimensional shapes created by thin sections cutting undeformed crinoid ossicles at different angles.

THEORY

For each of the two techniques, the rock to be analyzed should contain randomly oriented crinoid ossicles. The original distribution does not have to be perfectly random, as the methods are appropriate whenever adequate numbers of each of the different cuts (described below) are present in any given thin section. Such a distribution is easily verified by visual inspection of each section in a sample, and may be characteristic of most crinoidal grainstones. Three dimensional strain can sometimes be calculated even when the ossicles are preferentially oriented, such as when the crinoid disks are parallel to bedding, but only if the two techniques are used in combination and one of the three mutually perpendicular sections is oriented parallel to the originally circular cross sections of the ossicles (see later discussion).

Both methods assume strain homogeneity, both within individual ossicles and between different ossicles in the same sample. Furthermore, if there is equal-volume homogeneous deformation of both ossicles and matrix, the measured strain will be that of the bulk rock deformation; otherwise, it may represent only one component of the total strain.

The shape of a crinoid ossicle visible in thin section depends on the relative orientations of the ossicle and the section. If an undeformed circular ossicle is considered, the following possible shapes result (Fig. 1): a section perpendicular to the cylinder axis produces a circle (cut I); one crossing the cylinder without cutting either end creates an ellipse (cut II; Figs. 2a & b), a section cutting only one end of the cylinder yields a half ellipse, or triangular shape (cut III, Fig. 2a), a section cutting the cylinder at both ends will, in the general case, produce a sub trapezoidal geometry, with two straight and parallel sides, and two slightly curved, non parallel sides (cut IV), a lengthwise cut passing close to the center of the ossicle creates a sub rectangular shape (cut V; Fig. 2b), and a section parallel to the cylinder axis yields a rectangle (cut VI; Fig. 2a). The two strain analysis techniques make use of these various shapes produced by the angular relationship between the thin section and the ossicles.

R_f/ϕ method

If the ossicles are randomly oriented, cuts I and II (Fig. 1) produce a set of initially elliptical markers that are also randomly oriented. The final axial ratios (R_f) and orientations (ϕ') can be measured, and these objects are thus suitable for analysis by the many R_f/ϕ techniques that have been developed: e.g. the original method of Ramsay (1967, pp. 202–211) and Dunnet (1969), the modified method of Lisle (1977), the algebraic computation of Shimamoto & Ikeda (1976), the orientation net method of De Paor (1988), and others. If there is a slight preferential orientation of the ossicles, the techniques presented by Elliott (1970) and Dunnet & Siddans (1971) may be appropriate.

The theories and assumptions underlying the various R_f/ϕ methods are not addressed here. For a discussion of the relative merits, the statistical validity, and the limitations of the different techniques, the reader is referred to the original literature.

Angular shear strain method

The shapes of cuts III, IV, V and VI (Fig. 1) contain angular relationships of known perpendicularity in the undeformed state (Fig. 3). In order to avoid ambiguities, the originally perpendicular lines are shown connecting midpoints of opposite sides, as these orthogonal relationships are valid even when marker corners are not perfect right angles (cuts III, IV and V). After deformation, all markers oriented at an angle to the principal finite strain directions will be distorted so that the originally orthogonal lines will no longer be perpendicular (Fig. 3). Measurement of the resulting angular shear strain on two or more markers of different orientations can thus be used to derive graphically the finite strain using either the Breddin graph (Breddin 1956a, Ramsay 1967, pp. 236–242, Ramsay & Huber 1983, pp. 127–149) or the Mohr circle (Ramsay 1967, pp. 236–242, Ramsay & Huber 1983, pp. 127–149).

A unique solution is determined when there are only

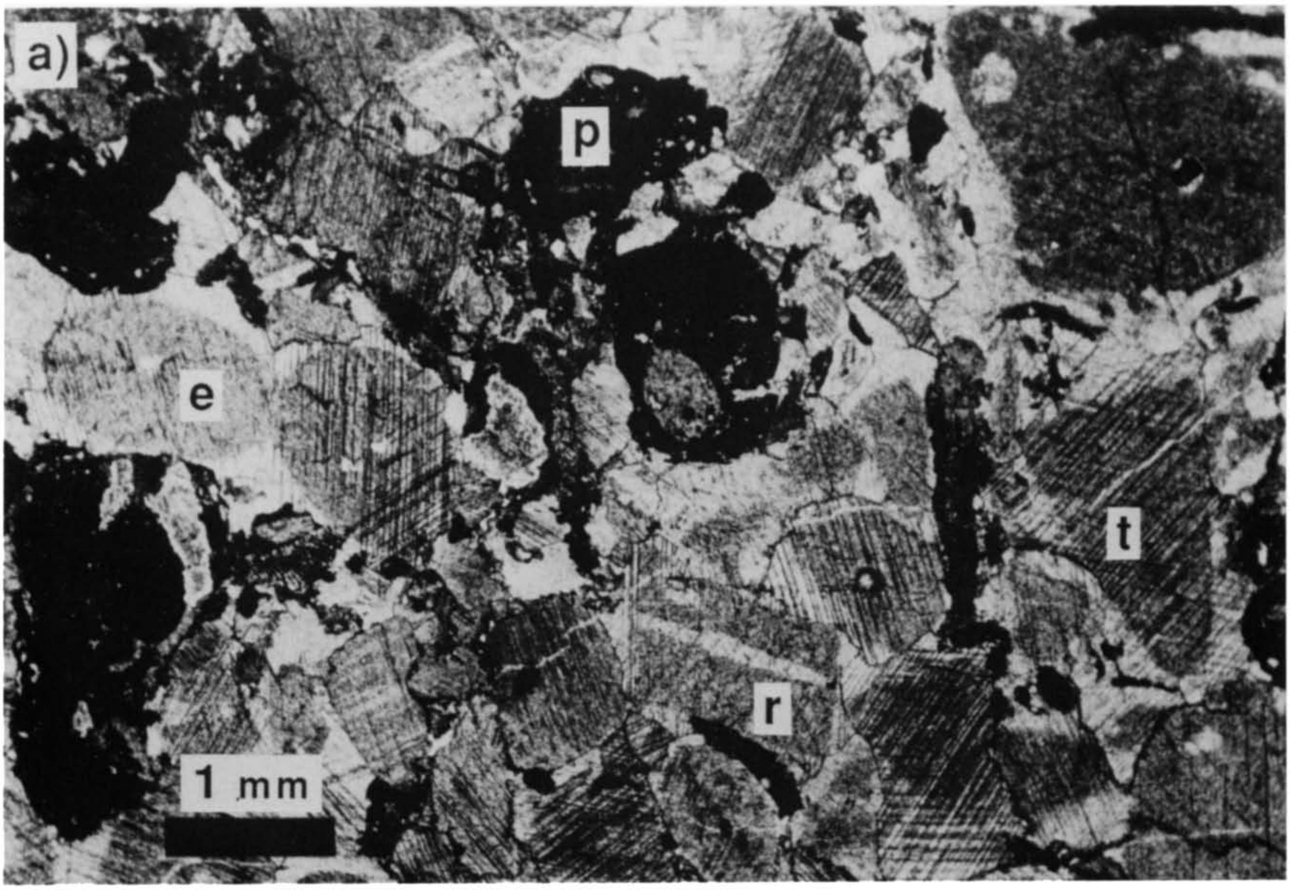

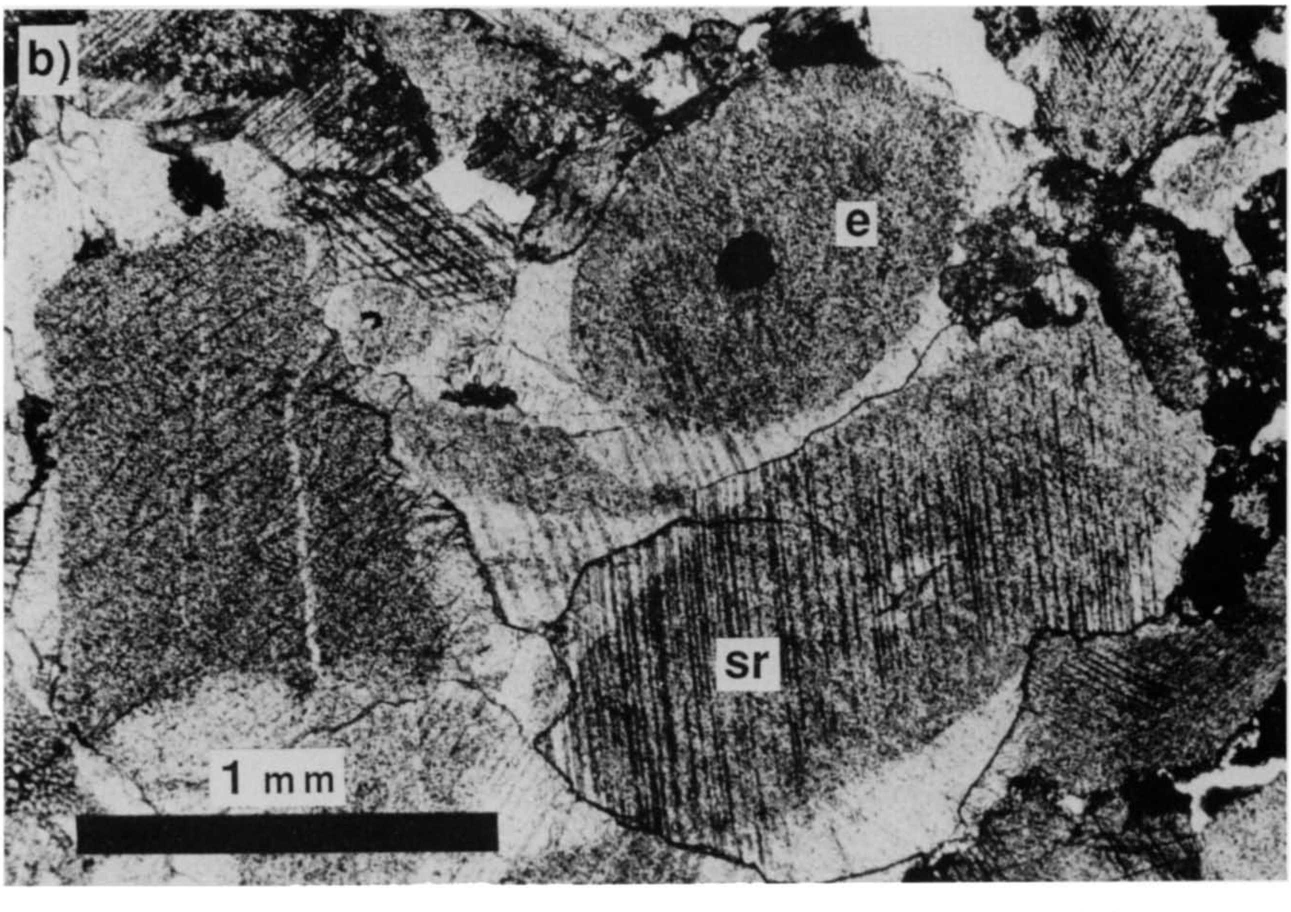

Fig. 2. Photomicrographs of Mid. Jurassic echinoderm grainstone from the Wildhorn Nappe, central Helvetic nappes, Switzerland. 'e'—elliptical (Type II) crinoid cuts; 't'—triangular (Type III) cut; 'sr'—sub-rectangular (Type V) cut; 'r'—rectangular (Type VI) cut; 'p'—micritic pellet. Note the optical continuity of crinoid grains (cloudy grey) and calcite spar cement (white), as shown by twinning.

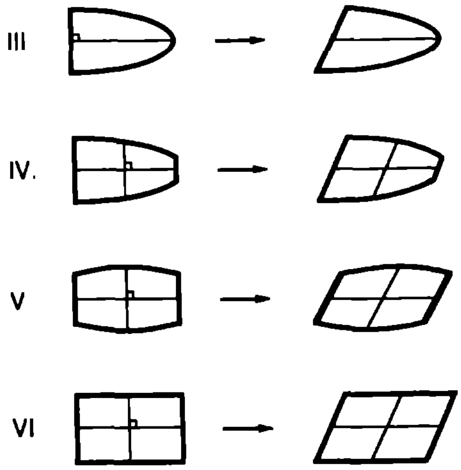

Fig. 3. Deformation of crinoid cuts III, IV, V and VI. Originally orthogonal lines develop angular shear strain.

two measurements of angular shear strain (this can also be calculated using the algebraic method of Ding 1984). However, in cases with more than two measurements and non homogeneous deformation, the data will rarely fall on a single curve, and the best-fit can be difficult to obtain. One approach is to apply a non linear least squares algorithm to the data. Rewriting an equation from Ramsay & Huber (1983, equation 8.5)

$$\gamma = (R^2 - 1)\tan(\theta - \beta)/(1 + R^2\tan^2(\theta - \beta)), \quad (1)$$

where γ is the shear strain, R is the axial ratio of the strain ellipse, θ is the angle between the shear strain direction and the chosen reference direction, and β is the angle between the maximum extension direction of the strain ellipse and the reference direction. The orientation (θ) and angular shear strain ($\psi = \tan^{-1}\gamma$) are measured for suitable markers, and equation (1) is solved for R and β using the Levenberg–Marquardt non-linear least-squares analysis (Press *et al.* 1988).

Using cuts III and IV (Fig. 1) for angular shear strain analysis can yield significant error, as the resulting deformed geometries may not have been derived from originally orthogonal relationships. *Pentacrinus* ossicles, either pentagonal or star shaped, are often found with normal cylindrical crinoids, and thin sections cut

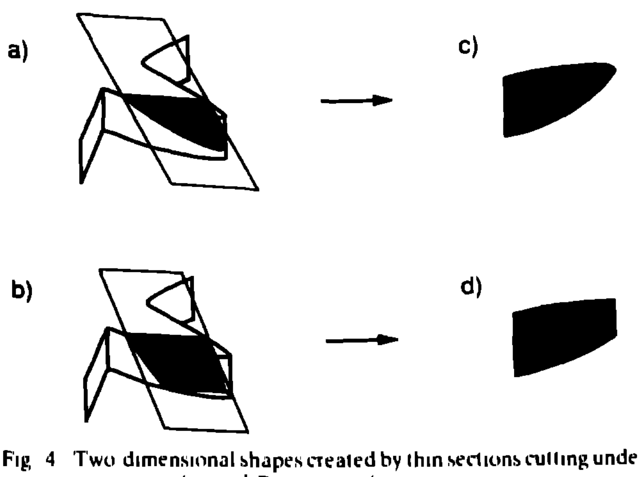

Fig. 4. Two dimensional shapes created by thin sections cutting undeformed *Pentacrinus* fragments.

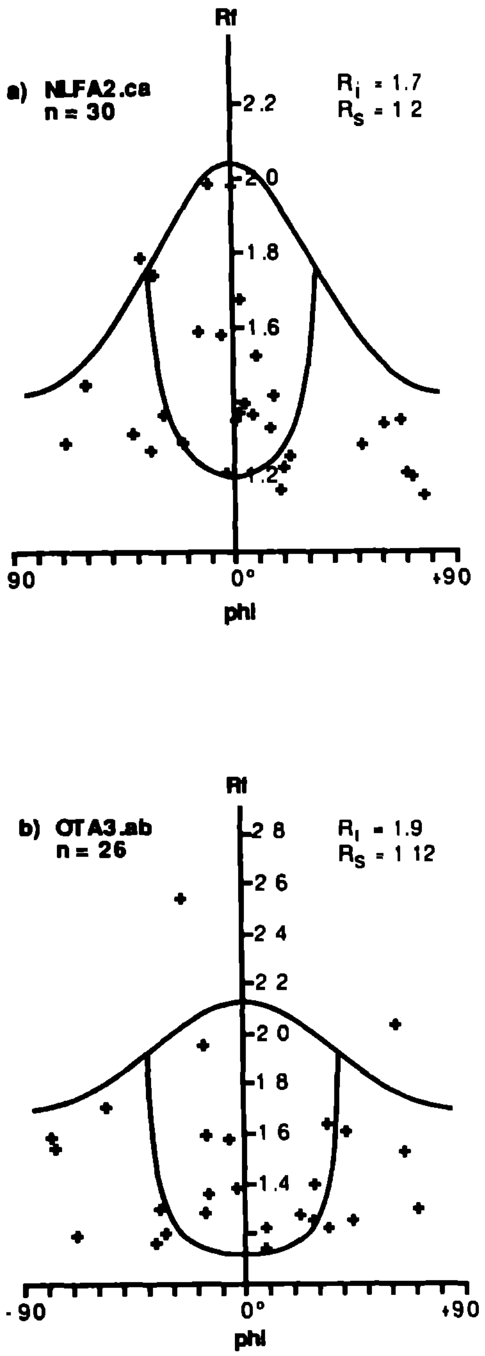

Fig. 5. Plots of R_f vs ϕ for samples (a) NLFA2.ca and (b) OTA3.ab. R_i is the maximum initial axial ratio, R_s is the axial ratio of the strain ellipse, n is the number of objects measured. The convex upward curve is the R_f/ϕ curve defined by R_i and R_s, and concave upward curve is the 50% data curve which divides the data into two equal halves. The principal direction (ϕ = 0) is the R_f weighted vector mean of marker orientations.

ting through an arm of an undeformed star shaped *Pentacrinus*, for example, can produce shapes that are similar to cuts III and IV (Fig. 4). These show an apparent angular shear strain (Figs. 4c & d), yet have undergone no deformation. Thus, strain analysis by the angular shear strain method should be confined to the sub-rectangular and rectangular shapes of cuts V and VI (Fig. 1), for which opposite sides are of the same length.

Another approach is possible using cuts V and VI, but has not been applied here. Roder (1977) has shown that

Table 1 Number of measured objects

Sample	All objects Fry	Crinoids R_i/ϕ	Crinoids Shear strain	Pellets R_i/ϕ
NLB1	250,231,222	59,51,33	3,4,3	90,65,59
NLB2	234,210,232	46,39,40	6,4,5	72,61,74
NLFA2	218,218,223	23,29,30	4,7,5	81,75,83
OTVA2	209,199,207	26,21,31	7,6,7	42,55,36
OTB	206,215,203	23,44,29	8,5,7	45,45,72
OTA3	184,217,205	26,31,38	6,5,4	31,45,41

Note Values are marker populations in each of three perpendicular sections

a unique ellipse can be inscribed within a parallelogram, so that these cuts may also be suitable for R_i/ϕ analysis One potential problem is created when undeformed ossicles have either high or low height-to-diameter ratios, and thus minimum initial axial ratios (R_i) substantially greater than 1 0 In these cases, a preferential original orientation of the markers may result in the calculation of excessively high strain ratios

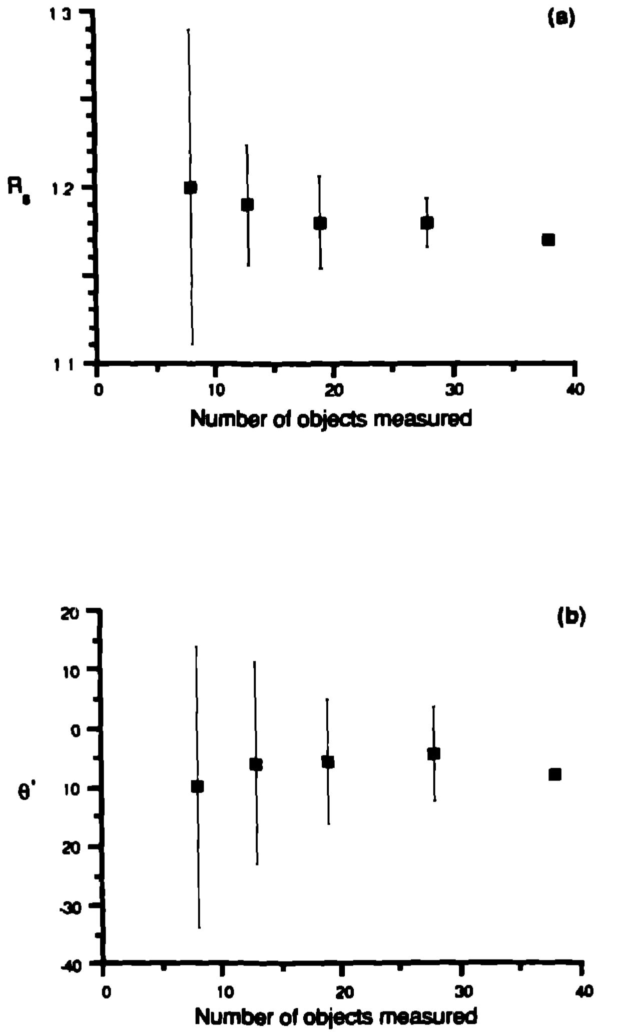

Fig 6 Determination of the strain ellipse as a function of number of objects measured for the standard R_i/ϕ method (a) axial ratio (R_s), (b) orientation of long axis (θ') Squares are mean values, bars represent one standard deviation

APPLICATION

The two strain analysis methods described above have been applied to six samples from the central Helvetic nappes of Switzerland. The samples are from the Echinoderm Member of the Middle Jurassic (Dogger) Hochstollen Formation and are situated on overturned folds of the Wildhorn Nappe in the area around the Faulhorn in the Berner Oberland between Grindelwald and Interlaken (see Rowan & Kligfield in press) The rock is a fine to very coarse grained echinoderm grainstone, dominated by crinoid ossicles and other echinoderm fragments, with minor amounts of predominantly micritic pellets and rare quartz grains, and cemented by a sparry calcite (Fig 2) Crinoid ossicles are single crystals of calcite, and the spar cement is in optical continuity with the grains (Fig 2b) The samples have no visible matrix and thus no grain matrix competency contrast (although the pellets form low competency inclusions) The measured strains are, therefore, assumed to approximate the bulk rock strain attributable to deformation mechanisms other than solution cleavage and dilatant veins spaced wider than the grain diameters

In the sections below, the results of the two methods are presented, with specific reference to individual two dimensional cuts through two different samples The examples have been chosen to illustrate the range of results obtained from relatively good data (sample NLFA2.ca) to relatively poor data (sample OTA3.ab). The calculated three dimensional strains from all six samples are then presented and compared to each other, as well as to those derived from R_i/ϕ analysis of the micritic pellets and all object Fry analysis (Fry 1979)

R_i/ϕ *methods*

Of the numerous variations of R_i/ϕ analysis available, three were chosen for application to the elliptical crinoid cuts the original method of Ramsay (1967, pp. 202–211) and Dunnet (1969), the unstraining ('theta curve') technique of Lisle (1977), and the algebraic computation of Shimamoto & Ikeda (1976)

The results of the original R_i/ϕ method are illustrated in Fig 5 Subjective best fit R_s/R_i curves for sample NLFA2 ca (Fig. 5a) are tightly constrained, whereas those for sample OTA3 ab (Fig 5b) are less well defined Both samples show symmetrical distributions of data points in the four curve quadrants, suggesting that the assumption of original random distribution is valid (Dunnet & Siddans 1971) Each is characterized by wide fluctuation (150° and 155°), high maximum initial ellipticities (1 7 and 1 9), and low tectonic strains (1 2 and 1 12); these values are representative of the suite of 18 analyzed sections. The Lisle (1977) unstraining and Shimamoto & Ikeda (1976) numerical methods produced almost identical results (see Table 2)

For elliptical crinoid cuts, the maximum initial axial ratio (R_i) is a function of the height to diameter ratio of the crinoidal columnals, and is produced by a thin section cutting diagonally from one corner of the disk to the opposite corner (steepest possible ellipse of type II, Fig 1) For crinoids of height h and diameter d

$$R_i = (d^2 + h^2)^{1/2}/d \qquad (2)$$

Spratt (1987, pp. 45–47) measured the dimensions of 50 undeformed ossicles from North America and Europe, and determined a maximum height do diameter ratio of 0 45 1, corresponding to a maximum R_i of only 1 1 Yet the maximum R_i values determined by the R_f/ϕ analyses of the Wildhorn Nappe crinoids range from 1 7 to 2 4, with a mean of 2 1. This discrepancy can be resolved by measuring the rectangular (type VI) cuts visible in the thin sections. Of the many such cuts, 16 were found that cut along the length of the axial canal and thus show the true cross sectional shape of the ossicles ('r' in Fig 2a) The height to diameter ratios measured for these objects have a mean of 1 8 and a maximum of 2 1, consistent with the results of the R_f/ϕ analyses As ossicle dimensions vary between different crinoid species, those measured by Spratt (1987) are not representative of the species found in the Wilhorn Nappe samples

In applying R_f/ϕ techniques to crinoid ossicles, it is important that enough objects be measured to give statistically meaningful results Because of the size of the markers (generally 1-2 mm in diameter) and the low proportion of elliptical cuts within a given rock volume, large format thin sections (5 × 7 5 cm) were used and are recommended In the samples analyzed, the number of objects measured ranged from a low of 21 to a high of 59 (Table 1). In order to test the statistical consistency of the results presented here, the R_f/ϕ method was applied to different subsets of the total data set from a sample with 38 elliptical cuts five sets of eight markers, five sets of 13 markers, four sets of 19 markers, three sets of 28 markers and one set consisting of all 38 objects The resulting mean values and standard deviations of the strain ellipse magnitude (R_s) and orientation (θ') are plotted in Figs 6(a) & (b), respectively The graphs suggest that for marker population sizes of over 20 objects, the strain ellipse magnitude can be determined within ±0 025, and its orientation within ±10°, for marker populations of over 30 objects, the corresponding values are ±0 015 and ±7° As the strain magnitude is 1 17 for this sample, the potential errors are probably greater at lower measured strains

Angular shear strain method

Even using large format thin sections, rectangular and sub rectangular crinoid cuts suitable for angular shear strain analysis are rare, ranging from three to eight per sample (Table 1) This is partially due to the large height to diameter ratios in the Helvetic nappe crinoids; species with the dimensions measured by Spratt (1987) would have higher proportions of these cuts The low numbers are also due to the elimination of any objects with opposite sides of unequal length: although these may be otherwise appropriate markers that have undergone slight non homogeneous deformation, they may also represent cuts through *Pentacrinus* ossicles with original non orthogonal geometries, and are thus suspect

Figure 7 shows the results from the same two samples used to illustrate the R_f/ϕ analysis, plotted on Breddin graphs of angular shear strain (ψ) vs marker orientation (ϕ') Again, sample NLFA2 ca (Fig 7a) is tightly constrained for determination of both strain ellipse magni

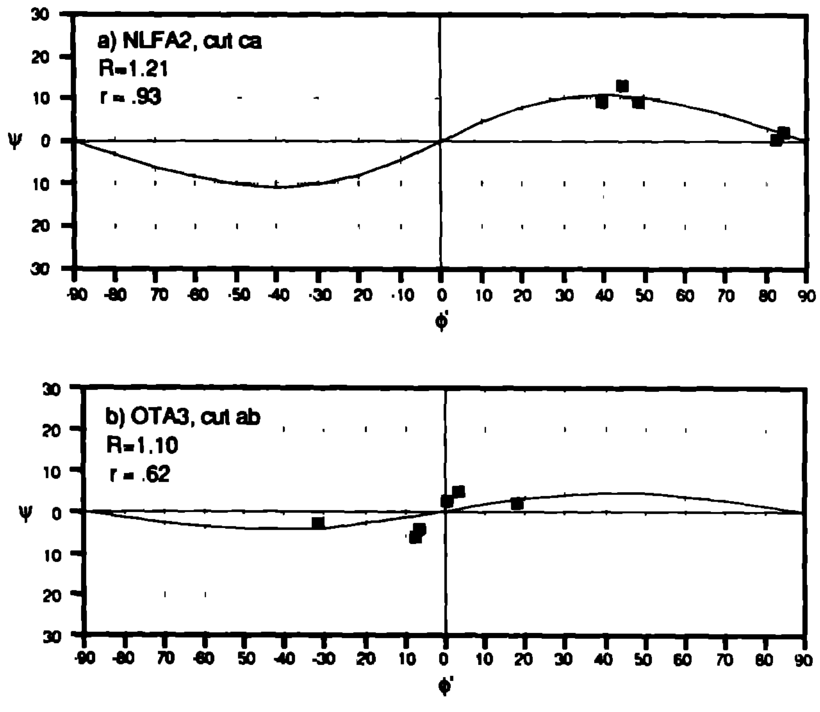

Fig 7 Breddin plots of angular shear strain (ψ) vs orientation (ϕ') for samples (a) NLFA2 ca and (b) OTA3 ab R is the axial ratio of the strain ellipse, squares are measured data The best fit curve is determined from a non linear least squares algorithm

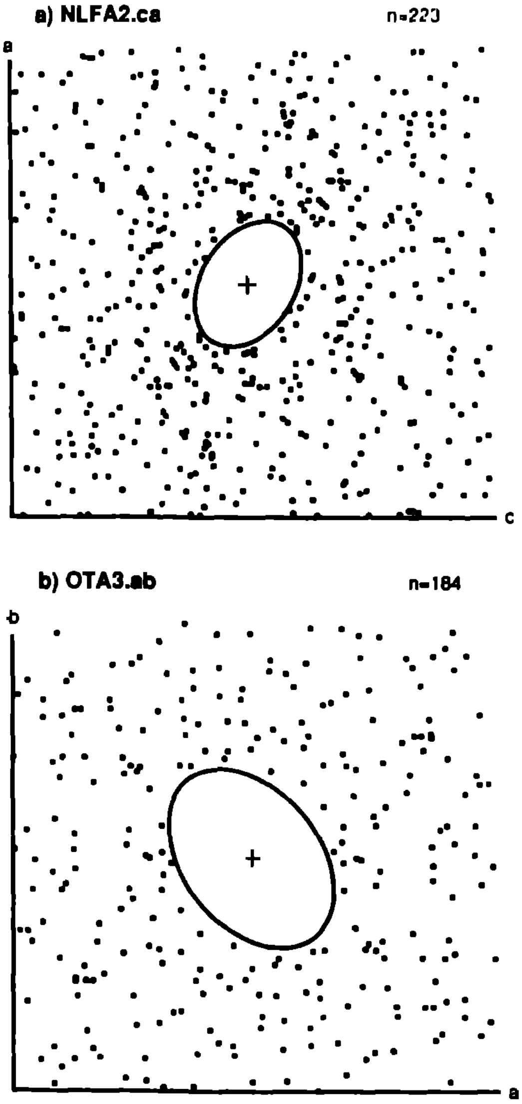

Fig. 8. Normalized (Erslev 1988) center to center Fry plots for samples (a) NLFA2.ca and (b) OTA3.ab. The shape and orientation of the inscribed strain ellipses were determined subjectively. *n* is number of objects.

tude and orientation, whereas sample OTA3.ab (Fig. 7b) shows considerable scatter of data around the best fit curve. The importance of the non linear least squares analysis of more than two markers is evident if the data from Fig. 7 are examined: matching a curve to only two markers (Breddin 1956a, Ramsay 1967, pp. 236–238, Ramsay & Huber 1983, pp. 127–149, Ding 1984) would yield widely discrepant results depending on which markers were selected. The scatter is most likely due to strain heterogeneities at the scale of the thin section.

Other methods

Two other strain analysis techniques were applied to the six samples for comparison with the results of the crinoid methods. First, the micritic pellets were analyzed by the same three R_f/ϕ techniques. These markers are more abundant than the elliptical crinoid cuts, ranging from 31 to 90 in the different samples (Table 1). The results were very similar to those derived from the R_f/ϕ analysis of the crinoids, though strain magnitudes were generally higher (see discussion below).

The second technique was the center to center method (Fry 1979), modified by the normalization procedure of Erslev (1988). All constituent objects of the samples were used, including the various crinoid shapes, other echinoderm fragments, quartz grains and pellets, with sample sizes ranging from 184 to 250 (Table 1). The results from the same two samples used to illustrate the crinoid methods are shown in Fig. 8, and again depict relatively good (Fig. 8a) and relatively poor (Fig. 8b) data.

Three dimensional strain

For each sample analyzed, and for each of the strain analysis methods, the results from three perpendicular sections were combined to generate the shape and orientation of the finite strain ellipsoid (Table 2) using the method of Owens (1984). As the results are difficult to evaluate in tabular form, the orientations of the principal axes of the strain ellipsoid are plotted on lower hemisphere, equal-area nets (Fig. 9), and the shapes of the ellipsoids are illustrated in a standard Flinn graph (Flinn 1962) (Fig. 10).

The orientations of the principal axes calculated from the different markers and the different two dimensional analyses are generally consistent (Fig. 9). There are two types of inconsistencies in the results: the first is simply scatter in the plotted positions of the axes, and the second is a switch of the X and Y axes for one analysis in four of the samples (NLB1, NLB2, NLFA2 and OTB). However, no systematic variation is apparent in that no one strain analysis method shows regular departures from the mean orientations, and the inconsistencies therefore are due probably to the inherent difficulties in determining accurately the magnitudes and orientations of the strain ellipse in samples with low strain.

The Flinn graph (Fig. 10) depicts the shapes and magnitude ratios of the strain ellipsoids, with most falling in the field of apparent flattening (Ramsay & Wood 1973). In contrast to the orientation data, the magnitude data show a systematic variation depending on the strain analysis method utilized. The R_f/ϕ and angular shear strain analyses of the crinoid ossicles record the lowest strains, with relatively low values of R_{xy} and R_{yz}, while the R_f/ϕ analysis of the pellets and the Fry analysis show intermediate and relatively high values, respectively. The pellets may have undergone greater deformation than the crinoids because of the lower competence of the micritic grains compared to the single crystal ossicles. The Fry analysis results are highest because the effects of grain to grain pressure solution were purposefully avoided in the shape analysis techniques by reconstructing and digitizing the uncorroded perimeters of the grains. As the micro scale bulk deformation is a product of the crystal plasticity, grain to grain pressure solution, and any grain boundary sliding, the shape analysis methods may, therefore, approximate the intracrystalline component of the finite

Table 2 Calculated strain ellipsoids

		All objects		Crinoids									Pellets					
		Fry		R_f/ϕ		Theta		Algebraic		Breddin			R_f/ϕ		Theta		Algebraic	
Sample	Axis*	Mag	Orient	Mag.	Orient	Mag	Orient	Mag	Orient	Mag.	Orient	Corr †	Mag	Orient	Mag	Orient	Mag	Orient
	X	1.12	04,259	1.12	17,058	1.14	16,058	1.09	14,055	1.19	34,338	0.61	1.17	10,052	1.18	09,051	1.15	09,051
NLb1	Y	0.98	17,168	0.97	07,326	0.98	09,325	0.99	08,323	0.99	01,247	0.86	0.99	01,322	1.01	01,321	1.02	03,321
	Z	0.84	72,003	0.92	72,216	0.89	71,206	0.92	74,205	0.85	56,155	0.66	0.86	80,228	0.84	81,227	0.85	81,214
	X	1.18	27,241	1.13	06,353	1.11	08,349	1.11	05,345	1.19	05,026	0.62	1.20	26,228	1.19	21,194	1.17	26,219
NLFa2	Y	1.03	04,332	1.01	19,261	1.01	19,256	1.01	18,253	1.01	40,291	0.87	1.06	07,321	1.04	21,292	1.05	11,314
	Z	0.82	62,069	0.88	70,100	0.90	69,101	0.89	71,091	0.83	50,121	0.93	0.79	63,065	0.81	60,063	0.81	61,065
	X	1.26	17,246	1.30	42,247	1.23	43,248	1.17	36,248	1.12	33,244	0.56	1.30	41,245	1.21	47,244	1.27	47,242
OTVa2	Y	1.04	73,077	1.10	47,057	1.12	47,059	1.12	54,060	1.03	57,068	0.99	1.05	48,078	1.10	43,078	1.06	42,078
	Z	0.75	03,337	0.70	05,153	0.72	05,153	0.76	04,155	0.87	02,335	0.78	0.73	07,341	0.75	07,342	0.74	08,341
	X	1.24	17,119	1.11	40,148	1.10	41,154	1.08	34,134	1.08	06,045	0.80	1.12	53,113	1.09	52,122	1.10	49,141
OTB	Y	0.97	42,225	1.02	02,057	1.02	04,060	1.01	06,228	1.02	32,138	0.78	1.05	02,021	1.06	06,025	1.05	13,035
	Z	0.83	43,012	0.89	51,325	0.89	49,326	0.92	56,327	0.91	57,305	0.89	0.85	37,289	0.87	38,291	0.87	38,294
	X	1.14	01,251	1.12	00,076	1.13	02,077	1.10	00,257	1.07	14,090	0.62	1.14	17,235	1.16	19,238	1.15	14,232
OTa3	Y	1.02	71,157	1.01	68,167	1.01	65,170	1.00	63,165	1.02	46,195	0.80	1.00	62,109	0.99	62,109	0.97	44,128
	Z	0.86	19,341	0.88	22,346	0.87	25,346	0.91	27,346	0.92	49,348	0.52	0.88	21,332	0.87	20,335	0.90	42,335
	X	1.15	15,174			1.06	06,240			1.12	06,241	0.83			1.11	05,226		
NLb2	Y	1.05	12,081			1.01	48,144			0.99	30,148	0.74			1.06	03,136		
	Z	0.82	71,314			0.93	41,335			0.90	59,342	0.77			0.85	85,018		

Note magnitude (Mag.) and orientation (Orient.) of strain ellipsoids calculated using method of Owens (1984). Fry—center-to-center method of Fry (1979). R_f/ϕ—method of Dunnet (1969). Theta—method of Lisle (1977). Algebraic—method of Shimamoto & Ikeda (1976). Breddin—angular shear strain method. Orientation is given as plunge and trend, in degrees.

* X, Y, Z are long, intermediate and short axes of strain ellipsoid.

† Correlation coefficients of the three two-dimensional sections (not ellipsoid axes) determined by the non-linear least-squares curve fitting.

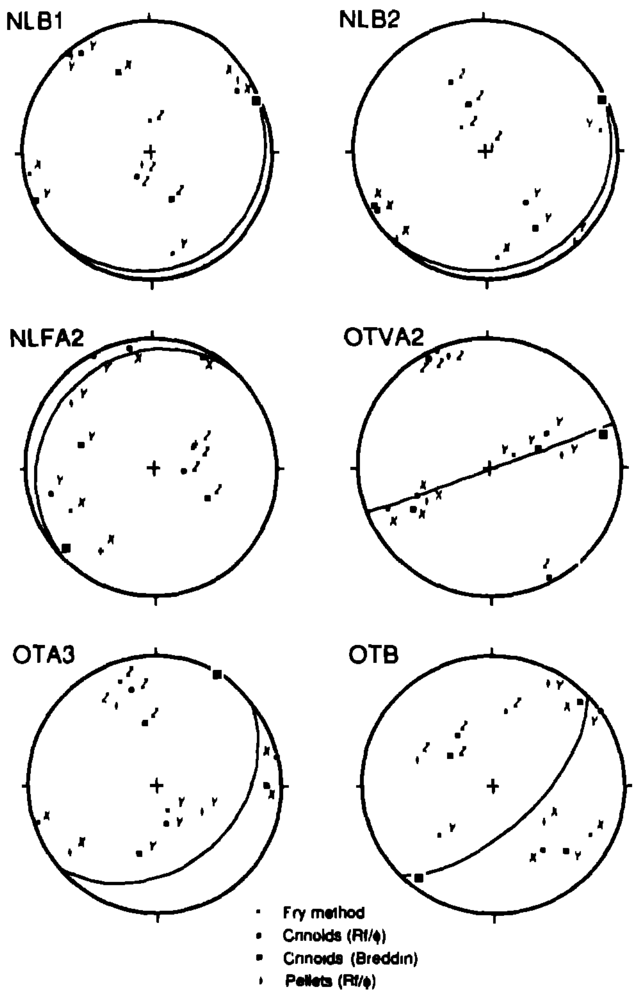

Fig 9 Lower hemisphere, equal area projections of the principal axes of the calculated strain ellipsoids X—long axis, Y—intermediate axis, Z—short axis For each sample, bedding is shown by the great circle, and the local fold axis by the solid square

strain, whereas the Fry analysis may record the total finite strain due to both crystal plasticity and grain to grain pressure solution The Fry analysis thus is a better indication of the bulk rock strain

DISCUSSION

The methods presented in this paper are simple extensions of well established strain analysis techniques When applied to crinoid ossicles from the Wildhorn Nappe, the methods produce results that are internally consistent and compatible with those from other strain analysis techniques The significant scatter and probable error ranges of the calculated strain ellipsoids are effects of the low strains in these samples, and would presumably be reduced at higher strain states

Although the techniques as described are applicable to rocks in which the crinoid ossicles are approximately randomly oriented, so that the different cuts of Fig. 1 are present in any thin section, the methods can be combined to measure three dimensional finite strain when the ossicles are preferentially oriented For example, if the crinoid disks lie approximately parallel to bedding (c axes orthogonal to bedding), three perpendicular thin sections should be cut so that one is parallel to bedding. The two-dimensional strain in this section is measured using R_f/ϕ analysis of the circular and elliptical cuts, and the other two sections, both oriented roughly parallel to the cylinder axes, are analyzed with the angular shear strain method on the rectanglar and sub rectangular cuts The results from the three sections are then combined as usual to calculate the finite strain ellipsoid. This technique will not work if the ossicles are all oriented identically, as the angular shear strain analysis will yield

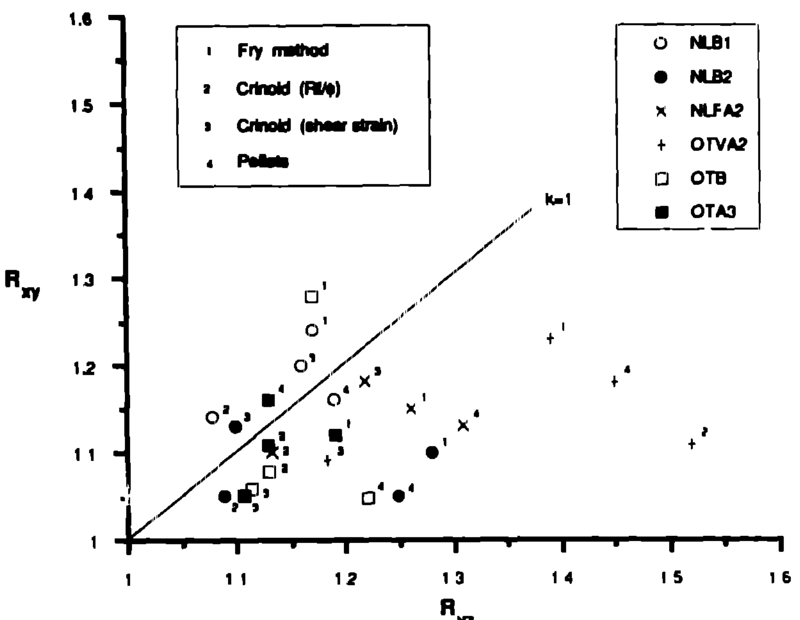

Fig 10 Flinn (1962) plot of strain ellipsoid shapes for each sample and strain analysis method R_{xy} is the ratio of X to Y principal axes, R_{yz} is ratio of Y to Z principal axes The k = 1 line divides the plot into regions of apparent flattening (right) and apparent constriction (left)

only one point on the Breddin graph, some variation in orientation is required. As the spread in orientations increases, the accuracy of the Breddin graph curve fitting also increases.

The methods described here have several advantages over the three dimensional technique developed by Spratt (1987). First, knowledge of the original shape of the ossicles, i.e. whether they had circular or elliptical cross-sections, is not required. The R_f/ϕ analysis is applicable in either case. Second, the orientations of the ossicle c axes do not need to be determined in order to remove the effects of oblique cuts through the crinoid disks. Third, the flat-stage technique for determining the c-axis orientations (Spratt 1987, pp. 48–57) is ambiguous for ossicles with large height to diameter ratios. Spratt showed that the c-axis cannot be determined uniquely if it is inclined between 26° and 64° to the pole of the thin section, and that since the elliptical cuts in her samples are always inclined at an angle of less than 24°, the method is useful. However, for ossicles with height-to-diameter ratios greater than 0.5:1, the c axis orientations cannot be determined unambiguously. In the case of the Wildhorn Nappe samples, the elliptical cuts may have c axes inclined up to 65° from the pole of the thin section, and the flat-stage technique is unusable. The R_f/ϕ and angular shear strain methods, on the other hand, are not bound by any of these restrictions, and can be applied easily to a wide range of crinoid-bearing rocks.

Acknowledgements—R. Kligfield is thanked for providing the opportunity to work in the Helvetic nappes, and R. Ratliff for first suggesting the analytical Breddin graph solution. Both also made helpful comments on the manuscript, as did G. Oertel, P. Hudleston, and an anonymous reviewer. Strain analyses were carried out in the Strain Analysis Microcomputer Laboratory at the University of Colorado, Boulder. Several programs are based on software originally designed by Roberts & Siddans (1971) and Peach & Lisle (1979). The research was supported by NSF grant EAR 86 16640 to R. Kligfield.

REFERENCES

Breddin, H. 1956a. Die tektonische deformation der fossilien im Rheinische Schiefergebirge. *Z. dt. geol. Ges.* **106**, 227–305.

Breddin, H. 1956b. Tektonische Gesteindeformation im Karbongurtel Westdeutschlands und Sudlimburgs. *Z. dt. geol. Ges.* **107**, 232–260.

Cloos, E. 1947. Oolite deformation in the South Mountain fold, Maryland. *Bull. geol. Soc. Am.* **58**, 843–918.

De Paor, D. G. 1988. R_f/ϕ_f strain analysis using an orientation net. *J. Struct. Geol.* **10**, 323–333.

Ding, Z. Y. 1984. Some formulae for calculating parameters of the strain ellipse. *Tectonophysics* **110**, 167–175.

Dunnet, D. 1969. A technique of finite strain analysis using elliptical particles. *Tectonophysics* **7**, 117–136.

Dunnet, D. & Siddans, A. W. B. 1971. Non random sedimentary fabrics and their modification by strain. *Tectonophysics* **12**, 307–325.

Elliott, D. 1970. Determination of finite strain and initial shape from deformed elliptical objects. *Bull. geol. Soc. Am.* **81**, 2221–2236.

Engelder, T. 1979. Mechanisms for strain within the Upper Devonian clastic sequence of the Appalachian Plateau, western New York. *Am. J. Sci.* **279**, 527–542.

Engelder, T. & Engelder, R. 1977. Fossil distortion and décollement tectonics of the Appalachian Plateau. *Geology* **5**, 457–460.

Erslev, E. A. 1988. Normalized center to center strain analysis of packed aggregates. *J. Struct. Geol.* **10**, 201–209.

Faill, R. T. 1977. Fossil distortion, Valley and Ridge Province, Pennsylvania. *Geol. Soc. Am. Abs. w. Prog.* **9**, 262–263.

Flinn, D. 1962. On folding during three dimensional progressive deformation. *Q. J. geol. Soc. Lond.* **135**, 291–305.

Fry, N. 1979. Random point distributions and strain measurement in rocks. *Tectonophysics* **60**, 89–105.

Hellmers, H. 1955. Crinoidenstielglieder als indikatoren der Gestein deformation. *Geol. Rdsch.* **44**, 87–92.

Kuttman, F. 1960. Fossildeformation und Tektonik im nordlichen Rheinischen Schiefergebirge. *Geol. Rdsch.* **49**, 439–459.

Lisle, R. J. 1977. Estimation of the tectonic strain ratio from the mean shape of deformed elliptical markers. *Geol. Mijnbouw* **56**, 140–144.

Moore, R. C. & Teichert, C. (editors) 1978. *Treatise on Invertebrate Paleontology, Part T, Echinodermata.* Geol. Soc. Am., Boulder, Colorado, and University of Kansas Press.

Nissen, H. U. 1964. Dynamic and kinematic analysis of deformed crinoid stems in a quartz graywacke. *J. Geol.* **72**, 346–360.

Oertel, G., Engelder, T. & Evans, K. 1989. A comparison of the strain of crinoid columnals with that of their enclosing silty and shaly matrix on the Appalachian Plateau, New York. *J. Struct. Geol.* **11**, 975–993.

Owens, W. H. 1984. The calculation of the best fit ellipsoid from elliptical sections on arbitrarily oriented planes. *J. Struct. Geol.* **6**, 571–578.

Peach, C. J. & Lisle, R. J. 1979. A Fortran IV program for the analysis of tectonic strain using deformed elliptical markers. *Comp. Geosci.* **5**, 325–334.

Press, W. H., Flannery, B. P., Teukolsky, S. A. & Vetterling, W. T. 1988. *Numerical Recipes in C.* Cambridge University Press, Cambridge.

Ramsay, J. G. 1967. *Folding and Fracturing of Rocks.* McGraw Hill, New York.

Ramsay, J. G. & Huber, M. I. 1983. *The Techniques of Modern Structural Geology, Volume 1: Strain Analysis.* Academic Press, London.

Ramsay, J. G. & Wood, D. S. 1973. The geometric effects of volume change during deformation processes. *Tectonophysics* **16**, 263–277.

Roberts, B. & Siddans, A. W. B. 1971. Fabric studies in the Llwyd Mawr Ignimbrite, North Wales. *Tectonophysics* **12**, 283–306.

Roder, G. H. 1977. Adaptation of polygonal strain markers. *Tectonophysics* **43**, T1–T10.

Rowan, M. G. & Kligfield, R. In press. Kinematics of large scale asymmetric buckle folds in overthrust shear: an example from the Helvetic nappes. In: *Thrust Tectonics* (edited by McClay, K.). Unwin Hyman, London.

Shimamoto, T. & Ikeda, Y. 1976. A simple algebraic method for strain estimation from deformed ellipsoidal objects. 1. Basic theory. *Tectonophysics* **36**, 315–337.

Siddans, A. W. B. 1980. Analysis of three dimensional, homogeneous, finite strain using ellipsoidal objects. *Tectonophysics* **64**, 1–16.

Spratt, D. A. 1987. Finite strain and deformation mechanisms in carbonate thrust sheets. Unpublished Ph.D. thesis, Johns Hopkins University.